



OPTIMIZATION OF THE RESISTANCE SPOT WELDING PROCESS OF SECC-AF AND SGCC GALVANIZED STEEL SHEET USING THE TAGUCHI METHOD



Sukarman^{1*}, Amri Abdulah¹, Apang Djafar Shieddieque¹, Nana Rahdiana², Khoirudin³

¹Mechanical Engineering Department, Sekolah Tinggi Teknologi Wastukencana, Indonesia

²Industrial Engineering Department, Universitas Buana Perjuangan Karawang, Indonesia

³Mechanical Engineering Department, Universitas Buana Perjuangan Karawang, Indonesia

Abstract

This article present the optimization work describes out to joint the dissimilar galvanized steel of SECC-AF (JIS G 3313) and SGCC (JIS G 3302) material. A zinc coating on the surfaces of the galvanized steel sheets will decrease the weldability characteristic of the material. This study used dissimilar galvanised steel sheets to obtain the highest tensile shear strength from the specified resistance spot welding. This research used the Taguchi method with 4-variables and mixed-experimental levels. The mixed-experimental level, namely 2-experimental levels for the first variable and 3-experimental levels for other variables. The highest tensile shear strength was achieved in 5282.13 N. This condition is achieved at a squeezed time of 20 cycles, 27 kA-welding currents, welding time of 0.5 seconds, and holding time of 18 cycles. The S/N ratio analysis has shown the welding current had the most significant effect, followed by welding time, squeeze time, and holding time. The delta values of S/N ratio were 0.79, 0.64, 0.26 and 0.07, respectively. The ANOVA analysis has shown that the P-value of welding current and welding time is 0.006 (0.6%) and 0.015 (1.5%), respectively. This result is expected for optimizing resistance spot welding quality in other materials or significant aspects.

This is an open access article under the [CC BY-NC](https://creativecommons.org/licenses/by-nc/4.0/) license



Keywords:

Dissimilar material;
Galvanized steel;
Resistance spot welding;
S/N Ratio;
Taguchi method;

Article History:

Received: November 5, 2020

Revised: January 5, 2021

Accepted: January 18, 2021

Published: August 25, 2021

Corresponding Author:

Sukarman

Mechanical Engineering
Department, Sekolah Tinggi
Teknologi Wastukencana,
Indonesia

Email: sukarman@stt-wastukencana.ac.id

INTRODUCTION

Resistance spot welding (RSW) is a process in which faying surfaces are joined in one or more spots by the heat-generated by resistance to the flow of electric current through workpieces held together under force by electrodes [1]. First, the pulse heats the contact surface in the area of current concentration (nugget) for a short time at low voltage. Then, a high electric current (ampere) is used to form nuggets so that the welding metal sticks together. The electrode force is maintained when the current flow stops, while the welding metal cools and hardens rapidly. The electrode is pulled after each welding process, which is usually completed in a fraction of a second [2].

Several welding techniques use resistance systems include Resistance Seam Welding (RSEW), Projection Welding (PW), Flash Welding (FW), Upset Welding (UW), Friction Stir Spot Welded, and Resistance Spot Welding (RSW) [3]. RSW is the most preferred and widely used method for sheet metal joining in automotive and many other industrial assembly operations [4]. That is understandable because RSW has many advantages. The advantages of the RSW technique include a stronger connection, ease to use, inexpensive, no filler required, and efficiency [5]. There are about 5000 points of spot welding on each unit car [6].

In general, spot welding is the most widely used joining technique for the assembly of sheet metal products. Consequently, it has been extensively used in many industrial fields, such as automotive body-in-white assemblies, domestic appliances, furniture, building products, enclosures, and, to a limited extent, aircraft [1][7].

The resistance spot welding (RSW) method provides electrical resistance as a heat source on two or more metal surfaces until fusion occurs in the welding area [8]. The molten metal in the welding area is formed due to the heat generated by the electric current's emergence of contact resistance. The connection is made by emphasizing the two surfaces of the plate be connected. The plate pressing process is performed using two electrodes throughout the RSW cycle (before, during, and after using the current).

The pressuring process in RSW aims to prevent the joint surface's deformation, forged the welded metal after heating, and ensure adequate contact between the welded parts [9] [10]. Welding current flows to both tips of electrodes caused contact metal surfaces to become melted. The melting process occurs when two adhesive metal surfaces melt together due to electrical resistance [9]. The stages of the welding cycle used in the study are pre-heat time, holding time without providing electricity, welding time, and hold-cooling. The detailed parameter settings for the eighteen iterations in the RSW schemes are shown in Table 1. The RSW cycle is presented in Figure 1 by studied [10].

Welding process resistance occurs when current flows across the electrode tip and the metal pieces to be joined. The base metal's resistance to the flow of electric current results in the joint (the nugget area/welding zone), resulting in the fusion between the two metals to be joined.

There are differences in the results of resistance spot welding with GTAW. The resistance spot weld is unique because the actual weld nugget is formed internally related to the surface of the base metal [8]. Figure 2 shows the difference between RSW and GTAW welding techniques [11][12].

Galvanized steel sheet has been widely used in the automobile industry. In Indonesia, about 80% of one million tons of galvanized steel material is used for the automotive industry [13]. Since 2018, the Indian government has required 80% of cars to use galvanized steel material [14]. Several types of galvanized steel materials are widely used in automotive industries, including SECC-AF and SGCC. Therefore, it is important to research the optimization of RSW parameters by using both materials.

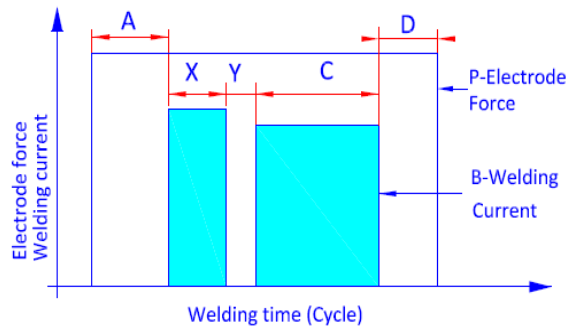


Figure 1. Spot welding scheme

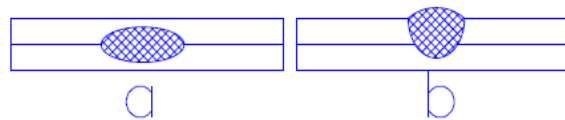


Figure 2. Schematic welding results (a) RSW and (b) GTAW

Table 1. Welding process parameters RSW scheme.

Parameters	Data Level experiments			Remarks
	I	II	III	
(A) Squeeze time (cycle)	20	22	-	Variable parameters
(B) Welding current (kA)	22	25	27	Variable parameters
(X) Pre-heat time (cycle)	4			Constant parameters
(Y) Holding time without applying current (cycle)	1			Constant parameters
(C) Welding time (second/cycle)	0.4/ 24	0.5/ 30	0.6/ 36	Variable parameters
(D) Holding and cooling time (cycle)	12	15	18	Variable parameters
(P) Electrode force (N)	68.7			Constant parameters

Several studies on RSW have been conducted include Thakur et al., 2014 [9]. The research was conducted by optimizing RSW parameters using galvanized steel sheets material. The optimization used the Taguchi method with 6-variables and 3-experimental

levels. The variables used current heating (kA), squeezing time (cycle), welding current (kA), welding time (cycle), resistance time (cycle), and pressure (MPa.). The significant parameters were analyzed with ANOVA.

The ANOVA results showed significant parameters that strongly affect the joint strength: the welding current and welding time. In contrast, the parameters of squeezing time and durability are less significant factors influencing the response variables [11]. Wan et al. researched the optimization of resistance spot welding used the titanium steel material. The research was conducted by the Taguchi method using 3-variables and 4-experimental levels.

The response variables used were a shear force, displacement in the peak load area, and nugget area. The input variables used are electrode force, welding current, and welding time. The optimum RSW parameter is obtained when the electrode force is 209.1 N, welding current in 1.83 kA, and welding time in 11.4 ms [12]. Vignesh et al. also conducted further research about the optimization RSW parameters process by joining two different materials, namely 316L austenite stainless steel and 2205 stainless steel. Optimization used the Taguchi method with 3-variables and 3-experiment levels. The variables input is electrode tip diameter (mm), the welding current (kA), and the heating cycle. Significant parameters were analyzed using ANOVA. The welding current is the most significant parameter to the tensile shear strength, followed by the heating cycle and the electrode tip diameter [15].

Li et al. (2018) improved resistance spot welding by adding a ring-shaped permanent magnet to improve austenitic stainless steels weld quality. Magnetically assisted resistance spot welding (MA-RSW) process proposed to improve the quality. The maximal peak force of MA-RSW increased by 8.9% compared to the RSW method. In addition, the hardness distribution inside the magnetically assisted weld nugget is more than that of a traditional weld nugget. As a result, the failure load of magnetically assisted resistance spot welds is higher and more stable than traditional ones [16]. Kim et al. (2019) conducted RSW for dissimilar spot welding between aluminum alloy (Al 6061-T6) and steel (GA440). The main variables used are electrode force, an 8-12 kA

welding current, the tensile shear strength, a 1.9-2.7 kN, and a 180-360 ms welding time. The strength of the dissimilar spot welds decreased with increasing force and increased in proportion to the weld time and current [17].

Unlike previous RSW process parameter optimization studied, this study was conducted using SECC-AF electro-galvanized material (JIS G 3313) and SGCC galvanized (JIS G 3303). It is important because differences in zinc layer thickness on RSW design parameters are still unclear. This paper continues previous research that successfully joined SECC-AF material with low carbon steel material [18]. This study aims to obtain the highest tensile shear strength test results from combining RSW process parameters to joining differences in the zinc layer thickness of galvanized steel. This study uses the Taguchi experimental method using four optimization variables/parameters. The optimization parameters to be used are squeeze time (cycle), welding time (cycle), welding current (kA), and holding time (cycle). This study used mixed experimental levels, namely 2-levels, for the first variable and 3-levels for the other variables.

METHOD

Material

SECC-AF and SGCC steel plate materials with a thickness of 0.8 mm each will be used in this study. Both materials are Zn-coated steel sheet plates that are widely used in the manufacturing industry. SECC-AF (JIS G 3313) material equivalent to ASTM A366-91 standard [19]. The zinc layer thickness for the material used in this study was 2.61 microns for SECC-AF and 12.75 microns for the SGCC material. The chemical composition of the SECC-AF steel sheet used in this study is shown in Table 2.

Table 2. Chemical composition of SECC-AF (%) steel sheet

Parameters	JIS G 3313 [20] [21]	C9AC3360A*
C	0.15 max.	0,0177
Mn	0,06 max.	0,0190
P	0,05 max.	0,0115
S	0,05 max.	0,0097

*Mill Test Certificate

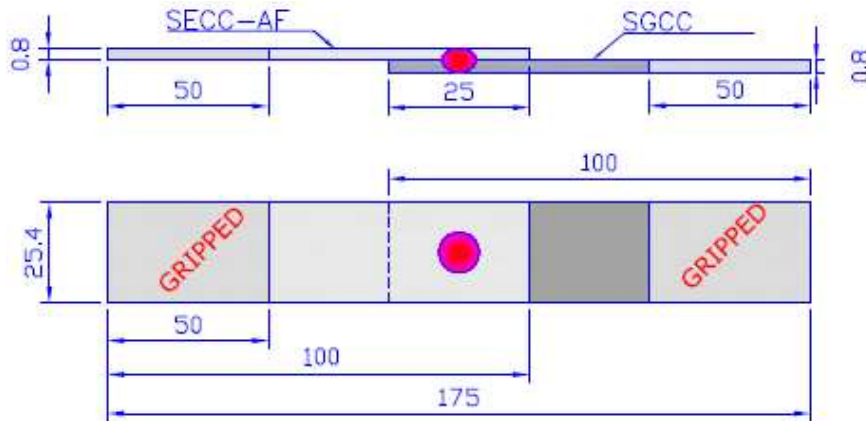


Figure 3. Specimen tensile shear strength - all dimensions are in mm [22]

Meanwhile, the mechanical properties of SECC-AF materials to be used in this study are shown in Table 3.

Table 3. Mechanical properties of SECC-AF steel sheet

SECC-AF	JIS G 3313 [20]	C9AC3360A*
YP (N/mm ²)	240 max.	216
TS (N/mm ²)	370 max.	316
EL (%)	30 min.	41
Coat. weight (gr/m ²)	18 min.	18,6
Thickness coating (μm)**	2.5 min	2.61

*Mill Test Certificate

**Thickness = coating weight/ density, zinc density = 7,14 gr/cm³

The chemical composition of SGCC steel plate according to JIS G 3302 and mill test certificate of material used in this experiment are presented in Table 4.

Table 4. Chemical composition of SGCC (%) steel sheet

Parameters	JIS G 3302 [23]	CSV4505B*
C	0.15 max.	0,0063
Mn	0,08 max.	0,1940
P	0,05 max.	0,0017
S	0,05 max.	0,0043

*Mill Test Certificate

Meanwhile, the properties of SGCC materials to be used in this study are shown in Table 5.

Table 5. Mechanical properties of SGCC steel sheet

Tensile test	JIS G 3302 [23]	CSV4505B*
YP (N/mm ²)	205 min.	231
TS (N/mm ²)	270 min.	333
EL (%)	-	45
Coat. weight (gr/m ²)	80.0 min.	91.0
Thickness coating (μm)**	11.2 min	12.75

*Mill Test Certificate

Specimens prepared by the cutting-shear process. At this stage, the 0.8 mm thick SECC-AF will be joined to the 0.8 mm SGCC steel sheet through the RSW process. The overlapping joining method will be used for a 25 x 100 mm coupon, according to ASTM D1002 [22]. The connection method is made overlapping with the dimensions, according to Figure 3.

Taguchi Experimental Design

RSW machine with a power capacity of 35 kVA will be used in this study. RSW machine is equipped with a pneumatic that is controlled at 3.5 MPa. The diameters of the top and bottom electrodes have 5 and 8 mm, respectively. The pneumatic force is used throughout the spot welding cycle. The following equation calculates pneumatic the compressive force at the end of the electrode [8].

$$F = P.A \tag{1}$$

Where F is the electrode force (N), P is the pressure (N/m²), and A is the cross-sectional area (m²). For example, with the electrode diameter above 5 mm, the force acting on the electrode can be calculated using equation one. The pneumatic force value is 68.7 N. The RSW machine used is shown in Figure 4.

RSW optimization used 4-variables: squeeze time in cycles, welding current in kA, welding time in seconds, and hold time in cycles. The mixed practical level design is presented in Table 6.



Figure 4. RSW machine 35 kW in capacity

Table 6. RSW parameters and their value for each level

Code	Weld. parameters	Level experiments		
		I	II	III
A	Squeeze time (cycles)	20	22	-
B	Weld. Current (kA)	22	25	27
C	Weld. Time (seconds)	0.4	0.5	0.6
D	Hold time (cycles)	12	15	18

$1 \text{ cycle} = \frac{1}{60} \text{ detik}$

Weldability material

The failure expected model for the RSW method is the pull-out failure model. Pull-out failure indicates that the strength of the connection is higher than the steel sheet connected. Generally, the RSW process has two failure models: pull-out failure mode and interfacial failure mode. The pull-out failure mode happened in two conditions. The first condition is the adequacy of the fusion between the related materials. The second condition is that the diameter of the electrode used must be achieved to minimum nugget diameter. The minimum nugget diameter is the smallest diameter that must be met. During the tensile shear test, the connection in the nugget area experiences a pull-out failure model. The minimum diameter required is determined by (2) [15][24].

$$D_{min} = 4.5\sqrt{t} \quad (2)$$

where t is the thickness of the smallest material to be joined. The SECC-AF and SGCC sheet steel materials have a thickness of 0.8 mm each. Therefore, using (2), the minimum diameter of the nuggets must be 4.27 mm. Furthermore, the tensile shear strength coupon will be processed with a 5.0 mm diameter electrode to fulfil these requirements.

Tensile shear strength

The tensile shear strength test aims to determine the tensile shear test's value for each parameter tested. The UTM used the Shimadzu AGS-X 10kN STD E200V model with having 10 kN in the capacity. The UTM testing was set and fixed at 35 mm/min. The tensile-share strength test process is shown in Figure 5.



Figure 5. Tensile-shear strength test of the coupon on UTM

Signal to Noise Ratio (S / N Ratio)

In the Taguchi experimental technique, the S/N ratio analysis is very important. The signal represents the desired value for the output (response variable). The noise represents the undesirable value for the output. This point indicates the best parameter that will give the highest or optimal tensile shear strength [25].

The calculation of the S / N ratio depends on the quality characteristics of the data being targeted. Taguchi provides the quality characteristics data into three parts, and it can be calculated with (3), (4), and (5) [17, 25, 26]. Smaller is better:

$$S/N \text{ ratio} = -10 \log \sum_{i=1}^{n_0} \frac{y_i^2}{n_0} \tag{3}$$

Larger is better:

$$S/N \text{ ratio} = -10 \log \frac{1}{n_0} \sum_{i=1}^{n_0} \frac{1}{y_i^2} \tag{4}$$

Nominal is the best:

$$S/N \text{ ratio} = -10 \log \frac{\bar{y}^2}{s^2} \tag{5}$$

Where n , y , \bar{y} , and s are the number of samples, response factor, mean response factor, and variance of the response factor. This study used the S/N ratio with characteristic data larger is better. A measurable S/N ratio characteristic with a non-negative value with an infinite ideal value.

These characteristics can be used to analyze other response data, such as tensile-shear strength [18], building strength [27], welding strength [28], corrosion resistance [29], tenacity of yarn [30], and fuel consumption. The S/N ratio for each L18 experiment has been calculated and listed in Table 7.

RESULTS AND DISCUSSION

Tensile-shear strength analysis

Table 7 shows that the highest tensile-shear strength was achieved in 5282.13 N. The optimum parameters were achieved in eight experiments with the pull-out failure model. The optimum parameters are squeeze time in 20 cycles, welding current in 27 kA, welding time in 0.6 seconds and holding time in 18 cycles. The graph of the tensile shear strength test is presented in Figure 6.

The pull-out failure mode was observed in all parameters of the welding time of 0.5 and 0.6 seconds. Meanwhile, when using the welding time of 0.4 seconds, it looks inconsistent and found the interfacial failure model. Two of the eighteen samples had interface failure modes. It was found in the 7th and 10th experiments of the sample. Both samples used a welding time of 0.4 seconds. They appeared to be an inconsistency of the fusion results in the nugget area. The experimental parameters for these failures are listed in Table 8.

Table 7. L18 orthogonal array of the experiments

Experiment	Parameter RSW				Tensile-shear test (N)	SNRA1	MEAN1
	Squee. Time (Cycle)	Weld. Current (kA)	Weld. Time (Second)	Hold time (Cycle)			
1	20	22	0.4	12	4345.21	72.76	4345.21
2	20	22	0.5	15	4477.02	73.02	4477.02
3	20	22	0.6	18	4463.24	72.99	4463.24
4	20	25	0.4	12	4547.20	73.15	4547.20
5	20	25	0.5	15	4725.49	73.49	4725.49
6	20	25	0.6	18	4902.22	73.81	4902.22
7	20	27	0.4	15	4485.42	73.04	4485.42
8	20	27	0.5	18	5282.13	74.46	5282.13
9	20	27	0.6	12	4936.09	73.87	4936.09
10	22	22	0.4	18	4224.74	72.52	4224.74
11	22	22	0.5	12	4626.24	73.30	4626.24
12	22	22	0.6	15	4988.25	73.96	4988.25
13	22	25	0.4	15	4786.88	73.60	4786.88
14	22	25	0.5	18	4899.33	73.80	4899.33
15	22	25	0.6	12	4922.74	73.84	4922.74
16	22	27	0.4	18	4876.82	73.76	4876.82
17	22	27	0.5	12	4989.75	73.96	4989.75
18	22	27	0.6	15	5133.60	74.21	5133.60

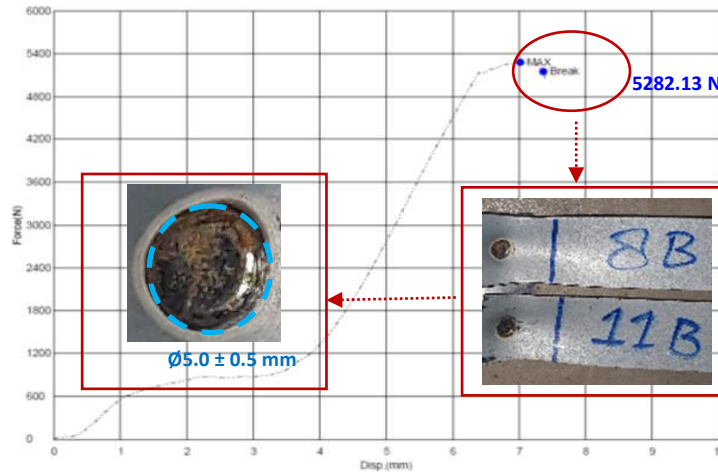


Figure 6. Tensile-shear for 8-experimental

Table 8. Interfacial failure mode parameters

Squee. time (Cycle)	Weld. current (kA)	Weld. time (Second)	Hold time (Cycle)
20	27	0.4	15
22	22	0.4	18



Figure 7. Interfacial Failure Mode

The interfacial failure mode that occurred in this study is presented in Figure 7.

S/N Ratio Analysis

S/N ratio analysis was performed to measure input variables' effect on the response variable's output. The input variables are the parameter process of resistance spot welding. The output or response variable is the tensile shear test. Figure 8 shows that the S / N ratio chart of lager is better characteristics, calculated using equation 5. The highest S / N ratio was achieved in the squeeze time in level-2, welding current in level-3, level-3, and holding time in level-3. It is also explained in the response table for S/N ratios of tensile shear strength in Table 9. Table 9 show that the highest tensile shear strength was achieved at the squeeze time in level-2, the weld current in level-3, welding time in level-3, and hold time in level-3. At the same time, the parameter that is most significant in the variable response in the combination of SECC-AF and SGCC materials using the resistance spot welding method is welding current with a

delta value of 0.79. The welding time delta values, squeeze time, and holding time parameters are 0.64, 0.26, and 0.07, respectively.

Figure 9 show the chart for the main effect of the mean tensile shear strength. The chart looks similar to the main effects plot for the mean because the data is linear to the S/N ratio. Table 7 describes the relationship between the mean and S/N ratio. For the mean of tensile shear strength, welding time and welding current have a higher delta value than other parameters. It means both variables have a more significant parameter effect on the response than others. In this case, welding current and welding time are the variables that most influence the output with delta values of 430 and 347. The delta values parameters for squeezing time and holding time are 143 and 47, respectively. Table 10 lists the mean response table for tensile shear strength at each RSW parameter.

Table 9. Response table for S/N ratios

Level	Squee. time (Cycle)	Weld. current (kA)	Weld. time (Second)	Holding time (Cycle)
1	73.40	73.09	73.14	73.48
2	73.66	73.62	73.67	73.55
3		73.88	73.78	73.56
Delta	0.26	0.79	0.64	0.07
Rank	3	1	2	4

Table 10. Response table for mean

Level	Squee. time (Cycle)	Weld. current (kA)	Weld. time (Second)	Holding time (Cycle)
1	4685	4521	4544	4728
2	4828	4797	4833	4766
3		4951	4891	4775
Delta	143	430	347	47
Rank	3	1	2	4

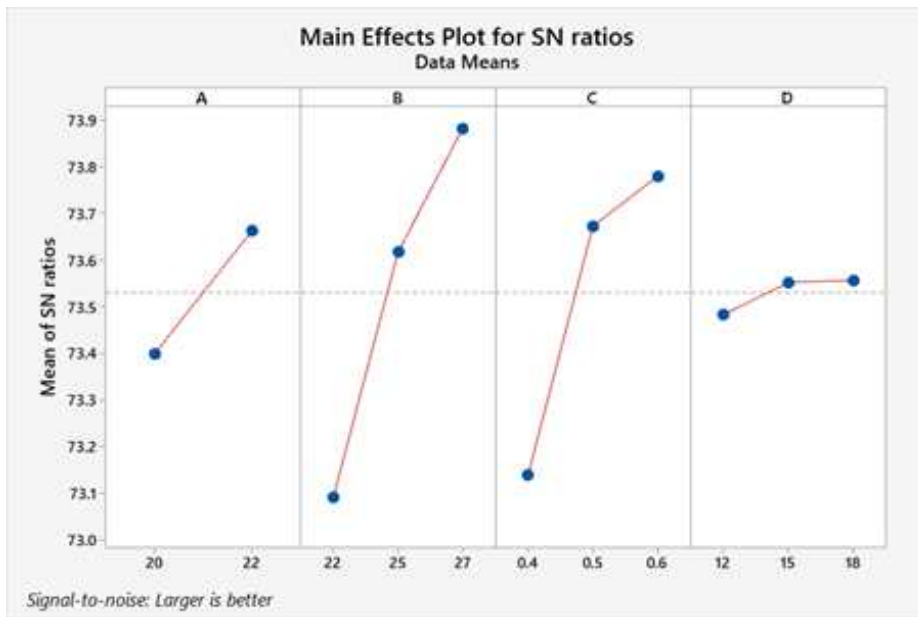


Figure 8. Main effect plot S/N ratio of the tensile shear strength

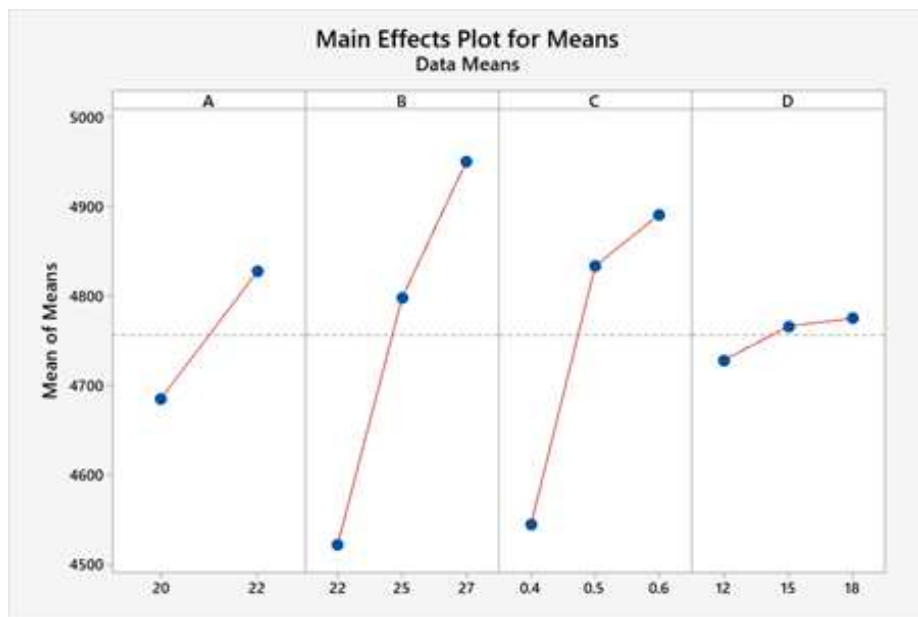


Figure 9. Main effects plot for the mean of tensile-shear stress

ANOVA Analysis

The S/N Ratio analysis provides the significance of a parameter compared to others on the response variable effect. Meanwhile, ANOVA analysis delivers data of significant parameters on the response variable [31]. ANOVA analysis was carried out using statistical software by setting the confidence level at 95%. The parameters with a P-value of equal or less than 5% significantly affect the variable response [25][31]. Although there are still have interfacial mode failures, this study has confirmed to the previous studies conducted by Thakur et

al. [11], Wan et al. [12], and Vignesh et al. [15] that welding current and welding time are parameters significantly affect the tensile shear strength.

Table 11 shows that variable welding current (source B) and welding time (source C) significantly affect the variable response. Meanwhile, the two other variables did not significantly influence the response variable. The P-value of welding current and welding time are 0.006 (0.6%) and 0.015 (1.5%), respectively. The ANOVA Analysis results are listed in Table 11.

Table 11. Analysis of Variance

Source	DF	Adj SS	Adj MS	F-Value	P-Value
A	1	91639	91639	2.94	0.117
B	2	569496	284748	9.12	0.006
C	2	413966	206983	6.63	0.015
D	2	7468	3734	0.12	0.889
Error	10	312217	31222		
Total	17	1394785			

CONCLUSION

Adjusting the right parameters in the resistance spot welding process involving PFS, especially spots welding for galvanized materials, has proven successful. Welding time and welding current have a significant effect on tensile shear strength. The highest tensile shear strength was achieved in 5282.13 N. For the optimum result, Taguchi suggests the squeeze time parameter in level-2, the weld current in level-3, welding time in level-3, and hold time in level-3. Further research will be carried out by looking at the zinc layer thickness's effect on tensile-shear strength and nugget diameter.

ACKNOWLEDGMENT

Thanks to the Ministry of Research, Technology & Higher Education Republic of Indonesia, who has fully funded this research through the Young Lecturer Research program with contract number 078/SP2H/LT-MONO/LL4/2020.

REFERENCES

- [1] D. L. Olson, S. Thomas A., S. Liu, and G. R. Edwards, *ASM Handbook Volume 6: Welding, Brazing, And Soldering*, ASM International, 2019
- [2] H. Wiryosumarto and T. Okumura, *Teknologi Pengelasan Logam*, 8th Ed. Jakarta: PT Pradnya Paramita, 2000
- [3] A. Armansyah and H. H. Chie, "Optimization of Process Parameters on Tensile Shear Load of Friction Stir Spot Welded Aluminum Alloy (Aa5052-H112)," *SINERGI*, vol. 22, no. 3, pp. 185-192, 2018, doi: 10.22441/sinergi.2018.3.007
- [4] A. H. Ertas and F. O. Sonmez, "Design optimization of spot-welded plates for maximum fatigue life," *Finite Elements in Analysis and Design*, vol. 47, no. 4, pp. 413-423, 2011, doi: 10.1016/j.finel.2010.11.003
- [5] M. P. Mubiayi, E. T. Akinlabi, and M. E. Makhatha, "Current Trends in Friction Stir Welding (FSW) and Friction Stir Spot Welding (FSSW)," *Springer International Publishing*, vol. 6, 2019, , doi: 10.1007/978-3-319-92750-3
- [6] S. H. M. Anijdan, M. Sabzi, M. Ghobeiti-hasab, and A. Roshan-ghiyas, "Materials Science & Engineering A Optimization of spot welding process parameters in dissimilar joint of dual phase steel DP600 and AISI 304 stainless steel to achieve the highest level of shear-tensile strength," *Material Science and Engineering: A*, vol. 726, no. April, pp. 120–125, 2018
- [7] B. Xing, Y. Xiao, Q. H. Qin, and H. Cui, "Quality assessment of resistance spot welding process based on dynamic resistance signal and random forest based," *The International Journal of Advanced Manufacturing Technology*, vol. 94, no. 1-4, pp. 327–339, 2018, doi: 10.1007/s00170-017-0889-6
- [8] NN, "Handbook for Resistance Spot Welding," *Miller Electric Manufacturing Co.*, 2012
- [9] P. Muthu, "Optimization of the Process Parameters of Resistance Spot Welding of AISI 316l Sheets Using Taguchi Method," *Mechanics and Mechanical Engineering*, vol. 23, no. 1, pp. 64–69, 2019, doi: 10.2478/mme-2019-0009
- [10] H. C. Lin, C. A. Hsu, C. S. Lee, T. Y. Kuo, and S. L. Jeng, "Effects of zinc layer thickness on resistance spot welding of galvanized mild steel," *Journal of Materials Processing Technology*, vol. 251, , pp. 205–213, March 2017, doi: 10.1016/j.jmatprot.2017.08.035
- [11] A. G. Thakur and V. M. Nandedkar, "Optimization of the Resistance Spot Welding Process of Galvanized Steel Sheet Using the Taguchi Method," *Arabian Journal for Science and Engineering*, vol. 39, no. 2, pp. 1171–1176, 2014, doi: 10.1007/s13369-013-0634-x
- [12] X. Wan, Y. Wang, and D. Zhao, "Multi-response optimization in small scale resistance spot welding of titanium alloy by principal component analysis and genetic algorithm," *The International Journal of Advanced Manufacturing Technology*, vol. 83, no. 1–4, pp. 545–559, 2016, doi: 10.1007/s00170-015-7545-9
- [13] K. Wibisono, "Pabrik baja galvanis KNSS pertama di Indonesia selesai 60 persen," *AntaraNews*, Jakarta, 2016
- [14] R. Mazumdar, "Government may force automakers to use 70 per cent galvanised steel in car body," *The Economic Times*, 2018
- [15] K. Vignesh, A. E. Perumal, and P. Velmurugan, "Optimization of resistance spot welding process parameters and microstructural examination for dissimilar welding of AISI 316L austenitic stainless

- steel and 2205 duplex stainless steel," *The International Journal of Advanced Manufacturing Technology*, vol. 93, no. 1-4, pp. 455–465, 2017, doi: 10.1007/s00170-017-0089-4
- [16] Y. B. Li, Q. X. Zhang, L. Qi, and S. A. David, "Improving austenitic stainless steel resistance spot weld quality using external magnetic field," *Science and Technology of Welding & Joining*, vol. 23, no. 8, pp. 1–9, 2018, doi:10.1080/13621718.2018.1443997
- [17] Y. G. Kim, D. C. Kim, and S. M. Joo, "Evaluation of tensile shear strength for dissimilar spot welds of Al-Si-Mg aluminum alloy and galvanized steel by delta-spot welding process," *Journal of Mechanical Science and Technology*, vol. 33, no. 4, pp. 5399–5405, 2019, doi: 10.1007/s12206-019-1034-2
- [18] S. Sukarman et al., "Optimization of Tensile-Shear Strength in the Dissimilar Joint of Zn-Coated Steel and Low Carbon Steel," *Automotive Experiences*, vol. 3, no. 3, pp. 115–125, 2020, doi: 10.31603/ae.v3i3.4053
- [19] N. T. Williams and J. D. Parker, "Review of resistance spot welding of steel sheets: Part 1 - Modelling and control of weld nugget formation," *International Materials Reviews*, vol. 49, no. 2, pp. 45–75, 2004, doi: 10.1179/095066004225010523
- [20] NN, "Japanese Standards Association," *JIS G 3313 Electrolytic zinc-coated steel sheet and coils*. pp. 428–480, 1998
- [21] D. Prayitno and A. Abyan, "Effect of Hot Dipping Aluminizing on The Toughness Of Low Carbon Steel," *SINERGI*, vol. 25, no. 1, pp. 75–80, 2021, doi: 10.22441/sinergi.2021.010
- [22] NN, "ASTM D1002 Standard Test Method for Apparent Shear Strength of Single-Lap-Joint Adhesively Bonded Metal Specimens by Tension Loading (Metal-to-Metal)," *ASTM International*, 2019
- [23] NN, "JIS G 3302 Hot-dip zinc-coated steel sheet and strip." *Japanese Industrial Standard*, 2007
- [24] S. T. Pasaribu, S. Sukarman, A. D. Shieddieque, and A. Abdulah, "Optimasi Parameter Proses Resistance Spot Welding pada Pengabungan Beda Material SPCC," *Seminar Nasional Teknologi Dan Riset Terapan (SEMNASTERA) 2019*, Jakarta, Indonesia, September 2019
- [25] S. F. Arnold, Design of Experiments with MINITAB, *The American Statistician*, vol. 60, no. 2. 2006, doi: 10.1198/tas.2006.s46
- [26] S. D. Sabdin, N. I. S. Hussein, M. K. Sued, M.S. Ayob, M.A.S.A Rahim, and M.Fadzil, "Effects of ColdArc welding parameters on the tensile strengths of high strength steel plate investigated using the Taguchi approach," *International Journal of Mechanical Sciences*, vol. 13, no. 2, pp. 4846-4856, 2019, doi: 10.15282/jmes.13.2.2019.06.0403
- [27] C. Jithendra and S. Elavenil, "Influences of Parameters on Slump Flow and Compressive Strength Properties of Aluminosilicate Based Flowable Geopolymer Concrete Using Taguchi Method," *Silicon*, vol. 12, no. 3, pp. 595–602, 2020, doi: 10.1007/s12633-019-00166-w
- [28] A. Abdulah, S. Sukarman, C. Anwar, A. Djafar Shieddieque, and A. Ilmar Ramadhan, "Optimization of yarn texturing process DTY-150D/96F using taguchi method," *Technology Reports of Kansai University*, vol. 62, no. 4, pp. 1471–1479, 2020
- [29] A. Farzaneh, M. Ehteshamzadeh, and M. Mohammadi, "Corrosion performance of the electroless Ni-P coatings prepared in different conditions and optimized by the Taguchi method," *Journal of Applied Electrochemistry*, vol. 41, no. 1, pp. 19–27, 2011, doi: 10.1007/s10800-010-0203-x
- [30] A. Budianto, S. B. Jumawan, and A. Abdulah, "Optimasi Respon Tunggal Pada Proses Texturing Benang Dty-150d / 96f Menggunakan Metode Taguchi Single Response Optimization Of Dty-150d / 96f Yarn Texturing Process using Taguchi Method," *Arena Tekstil*, vol. 35, no. 2, pp. 77–86, 2020
- [31] E. Del Castillo, *Process Optimization A Statistical Approach*. Springer, New York, UK, 2007